Service Science

Publication details, including instructions for authors and subscription information:
http://pubsonline.informs.org

Airplane Seating Assignment Problem

John A. Pavlik, Ian G. Ludden, Sheldon H. Jacobson, Edward C. Sewell

To cite this article:
John A. Pavlik, Ian G. Ludden, Sheldon H. Jacobson, Edward C. Sewell (2021) Airplane Seating Assignment Problem. Service Science 13(1):1-18. https://doi.org/10.1287/serv.2021.0269

http://pubsonline.informs.org/journal/serv

SERVICE SCIENCE
Vol. 13, No. 1, March 2021, pp. 1–18
ISSN 2164-3962 (print), ISSN 2164-3970 (online)

Airplane Seating Assignment Problem

John A. Pavlik,[a] Ian G. Ludden,[a] Sheldon H. Jacobson,[a] Edward C. Sewell[b]

[a] Department of Computer Science, University of Illinois at Urbana–Champaign, Urbana, Illinois 61801; [b] Department of Mathematics and Statistics, Southern Illinois University Edwardsville, Edwardsville, Illinois 62025

Contact: jpavlik2@illinois.edu, https://orcid.org/0000-0002-5662-4117 (JAP); iludden2@illinois.edu, https://orcid.org/0000-0002-5913-1123 (IGL); shj@illinois.edu, https://orcid.org/0000-0002-9042-8750 (SHJ); esewell@siue.edu (ECS)

Received: October 15, 2020
Revised: December 1, 2020; January 10, 2021
Accepted: January 15, 2021
Published Online in Articles in Advance: March 16, 2021

https://doi.org/10.1287/serv.2021.0269

Abstract. SARS-CoV-2, the virus that causes COVID-19, began infecting humans in late 2019 and has since spread to over 57 million people and caused over 1.75 million deaths, as of December 27, 2020. In response to reduced demand and travel restrictions as a result of COVID-19, airlines experienced a 94% reduction in passenger capacity worldwide in April and an estimated 60% reduction in passengers transported for all of 2020. SARS-CoV-2 has been shown to spread on airplanes by infected passengers, so minimizing the risk of secondary infections aboard aircraft may save lives. We present the airplane seating assignment problem (ASAP) to minimize transmission risks on airplanes, and we provide two models to solve ASAP. We show that both models can be effectively solved using a standard commercial solver and that seating assignments provided by these models have lower aggregate risk than the strategy of blocking the middle seats, given the same number of passengers. The available risk models for aircraft are based on influenza data, and hence risk models based on SARS-CoV-2 should be developed to maximize the benefits of our research.

Funding: I.G. Ludden's research has been supported by the National Science Foundation Graduate Research Fellowship Program [Grant DGE-1746047]. Any opinions, findings, and conclusions or recommendations expressed in this material are those of the author(s) and do not necessarily reflect the views of the National Science Foundation. S. H. Jacobson's research has been supported in part by the Air Force Office of Scientific Research [Grant FA9550-19-1-0106]. Any opinions, findings, and conclusions or recommendations expressed in this material are those of the authors and do not necessarily reflect the views of the United States Government, or the Air Force Office of Scientific Research.

Keywords: public health • air travel • COVID-19 • discrete optimization

1. Introduction

COVID-19 is a new respiratory disease caused by the SARS-CoV-2 virus. The first known case developed symptoms on December 1, 2019. On January 31, 2020, Secretary Alex Azar of the U.S. Department of Health and Human Services declared a public health emergency (Azar 2020), and President Donald Trump imposed travel restrictions on non-U.S. citizens traveling from China to the United States (Trump 2020). As of December 27, 2020, COVID-19 has killed over 1.75 million people worldwide and over 328,000 people in the United States (World Health Organization 2021).

Airports and airlines responded to COVID-19 with increased cleaning and sanitizing procedures, social distancing where possible, the use of face masks, temperature testing, and the protocol of asking passengers to self-report symptoms (Pombal et al. 2020). Airlines faced significant cancellations and travel restrictions from multiple countries in response to COVID-19, leading to sharp decreases in the number of flights and passenger capacity relative to a baseline year. By March, China was down 82%, Republic of Korea 70%, and Italy 60% of their respective airline passenger capacities. The estimate for the entire year of 2020 is a 60% worldwide reduction in total passengers and a 61% reduction in airport revenue as a result of COVID-19 (Air Transport Bureau 2020).

There are multiple instances of SARS-CoV-2 transmission reported between passengers on airplanes. After a flight from Singapore to Hangzhou on January 24, 2020, passengers were screened, and two passengers showed symptoms of fever and upper respiratory infection. All of the crew and passengers from that plane were placed into a 14-day quarantine. In total, 16 passengers from that flight tested positive for SARS-CoV-2 during quarantine, with 2 symptomatic during the flight and likely infectious. Thirteen had other potential sources of exposure before the flight, and hence they could have been infected either before or during the flight. One passenger was most likely infected during the flight, given that he had no other likely sources of exposure and spent at least one hour talking and eating near four other SARS-CoV-2-positive passengers, including one with symptoms during the flight (Chen et al. 2020, Yang et al. 2020).

On March 2, 2020, a flight from London to Hanoi carried a passenger experiencing a sore throat and cough symptoms. Her symptoms were not caught during screening, she did not self-report, and no quarantine was required for passengers from the United Kingdom at that time. Her symptoms worsened after arrival, and she tested positive for SARS-CoV-2 four days later. The passengers on that flight were traced, but 33 of them had already transited onto other countries and were not located or tested. Of the 168 passengers and 16 crew from the flight who were successfully traced, 15 passengers and 1 crew tested positive for SARS-CoV-2 (Khanh et al. 2020). If any of the passengers who could not be traced also were infected, then they may have continued to spread SARS-CoV-2 during their journey or at their final destinations.

Eight passengers were very likely infected during a flight on March 21, 2020, from Sydney to Perth. Genomic sequencing confirmed those 8 had a strain of the virus that was not circulating at their locations of origin, the United States and New South Wales. That same strain was being carried by 9 other passengers on the aircraft who later tested positive and were most likely infectious during the flight. Another 3 passengers were possibly infected during the same flight, for a total of 11 potential secondary infections on that flight (Speake et al. 2020).

Numerous flights with no reported secondary infections carried passengers who tested positive for SARS-CoV-2 (Freedman and Wilder-Smith 2020, International Air Transport Association 2020). Airplanes have several factors that lower the risk of transmitting SARS-CoV-2 between passengers, such as environmental control systems (ECS) that cycle air in the cabin every two or three minutes, HEPA filters, and passengers who have no face-to-face interaction during the flight (Embraer 2020, Fargeon 2020).

Given the dangers of COVID-19 to at-risk populations and the known cases of SARS-CoV-2 transmission aboard aircraft, minimizing the risk of transmitting SARS-CoV-2 between airplane passengers is ideal. We present the *airplane seating assignment problem* (ASAP): given an airplane cabin seating arrangement, assign passengers to seats minimizing the risk of spreading transmissible respiratory diseases such as influenza or SARS-CoV-2. An optimal solution for ASAP is a seating assignment that reduces the risk of secondary infections on aircraft and can be added to the aircraft's existing advantages to further reduce the risks of transmitting COVID-19. We provide two new formal problems, *vertex packing risk minimization* (VPR) and *risk-constrained vertex packing* (RCV), which model ASAP such that an optimal solution to VPR or RCV corresponds to an optimal seating arrangement.

Airlines have implemented COVID-19 mitigation seating strategies such as blocking middle seats (Delta Air Lines, Inc. 2020), limiting airplane capacity and allowing passengers to space themselves (Reuters 2020), or filling the middle seats last (Pallini 2020). We construct an instance of VPR or RCV matching the specific airplane being filled using the best-known disease transmission risks and then solve the instance to generate an optimal seating solution.

For both VPR and RCV, we model the airplane seating environment as an undirected graph. Every seat on the airplane corresponds to a single vertex in the graph. Edges between vertices represent the risk of transmitting a disease between each pair of seats. If either seat in a pair is empty, then there is no risk of transmitting a disease, and hence VPR and RCV are closely related to the vertex packing problem (also called the maximum independent set or stable set problem).

Given an undirected graph modeling an airplane seating assignment problem instance with appropriate risks on the edges, the solution to VPR is an optimal configuration of seats to minimize the risk of transmission for a fixed number of passengers on the airplane. Similarly, the solution to RCV is the maximum number of passengers and corresponding seat configuration given a maximum acceptable total risk of transmission.

The rest of this paper is organized as follows. Section 2 summarizes prior studies of related problems. Section 3 formulates VPR and RCV as integer programs. Section 4 defines risk models for assigning edge costs in the case of a respiratory disease on an airplane. Section 5 describes experiments solving VPR and RCV on different airplanes and summarizes the results.

2. Related Problems

Both VPR and RCV are extensions of the vertex packing problem. The vertex packing problem takes an input graph $G = (V, E)$ and selects a maximum cardinality vertex subset P such that for all $u, v \in P$, $uv \notin E$ (Nemhauser and Trotter 1975, Tarjan and Trojanowski 1977). In other words, the vertex packing problem selects the maximum number of vertices such that no two selected vertices share an edge. Let x_v represent a vertex indicator variable, where $x_v = 1$ if vertex v is included in the solution and 0 otherwise. The model for the vertex packing problem is

$$\begin{aligned} \text{maximize} \quad & \sum_{u \in V} x_u \\ \text{subject to} \quad & x_u + x_v \le 1 \quad \text{for all } uv \in E, \\ & x_u \in \{0, 1\} \quad \text{for all } u \in V. \end{aligned}$$

VPR and RCV extend vertex packing by relaxing the nonadjacency constraint and adding an edge cost function $c : E \to \mathbb{R}^+$ representing the risk of using

both vertices connected by the edge. VPR and RCV are formally defined in Section 3.

A similar problem to VPR and RCV that also extends vertex packing and has already been studied is the generalized independent set (GIS). Hochbaum and Pathria (1997) studied GIS in the context of forestry management, which was expanded in Hochbaum (2004). GIS extends the independent set (vertex packing) problem by assigning revenue to each vertex and cost to each edge and then selecting $P \subseteq V$, which maximizes the net profit of the induced subgraph (i.e., the sum of vertex revenues minus the sum of edge costs).

Given the independent set problem with the adjacency constraint removed, the only optimal solution is to include every vertex. GIS prevents the only solution from being to include every vertex by expanding the objective function to subtract edge costs when both vertices of the edge are included, penalizing solutions that contain excess vertices. However, subtracting edge costs assumes that vertices and edges have a comparable metric. For example, if the vertices are represented as profit and the edges as costs, with both measured in dollars, then the profit and costs are comparable, and a difference can be calculated. GIS is not applicable to a problem domain if no comparison metric exists, but VPR and RCV are applicable because they do not require such a metric. VPR constrains exactly the number of vertices required to be part of the solution, and RCV sets an upper bound on the sum of the edge costs.

GIS shares a structural similarity to VPR and RCV. As such, we consider GIS solutions to see whether they are also applicable to VPR and RCV. Kochenberger et al. (2007) studied and compared two approaches for solving GIS. Their first approach is a linear model using x_u as a binary decision variable to include vertex u in a solution subset S. Let w represent vertex weights, where the weights represent the profit or revenue of including the vertex in the solution; let c represent edge costs; and let z_{uv} be a binary variable that has value 1 if and only if there is an edge uv in E and both u and v are included in S. The resulting GIS linear model is

$$\begin{aligned} \text{maximize} \quad & \sum_{u \in V} w_u x_u - \sum_{uv \in E} c_{uv} z_{uv} \\ \text{subject to} \quad & x_u + x_v - 1 \le z_{uv} \quad \text{for all } uv \in E, \\ & x_u, z_{uv} \in \{0,1\} \quad \text{for all } u, v \in V. \end{aligned}$$

Kochenberger et al. (2007) solved the model using CPLEX 8.1 on test problems ranging in size from 50 to 400 vertices. The z_{uv} binary variable, representing edges with both vertices included, can be used to build linear models for the VPR and RCV problems.

Their second approach to solving GIS is a 0-1 quadratic model substituting $x_u x_v$ for z_{uv} in the maximization. This removes the z value and corresponding constraint, leaving only the binary restriction on x as a constraint. This nonlinear model was solved using a tabu search approach described in Glover et al. (1998, 1999). The tabu search results were faster than solving the linear model but had no guarantee of finding the optimal solutions, so we exclude this approach to solving VPR or RCV for the purposes of this paper. However, tabu search remains a potential alternative if fast but nonoptimal solutions are acceptable.

A related problem that also extends vertex packing is generalized vertex packing (GVP-k) (Sherali and Smith 2006). GVP-k relaxes the shared edge constraint and allows up to k shared edges in the solution. GVP-k has a similar linear formulation to GIS but does not factor in edge weights in the maximization, only *counting* edges that violate the shared constraint instead of assigning edge weights. The GVP-k linear model is

$$\begin{aligned} \text{maximize} \quad & \sum_{v \in V} c_v x_v \\ \text{subject to} \quad & \sum_{uv \in E} z_{uv} \le k, \\ & x_u + x_v - 1 \le z_{uv} \quad \text{for all } uv \in E, \\ & z_{uv} \ge 0, \quad \text{for all } uv \in E, \\ & x_v \in \{0,1\} \quad \text{for all } v \in V. \end{aligned}$$

More recently, Salari et al. (2020) studied passenger assignments to seats on an airplane based on social distancing and proximity to the aisle. They present two models. The first model (model 1) minimizes the number of passengers who are within social distancing guidelines of each other while also minimizing the number of passengers seated near the aisle. Model 1 is similar to VPR in that both models take a fixed number of passengers and try to assign an optimal seating assignment while using the same binary formulation as GIS and GVP-k. The difference between model 1 and VPR is in the objective function. VPR minimizes total risk as modeled by direct virus transmission probabilities, whereas model 1 minimizes (i) the number of passengers who are violating social distancing guidelines, as measured by Euclidean distance, and (ii) the number of passengers in aisle seats. Salari et al. (2020) also presented a second model (model 2) that maximizes the number of passengers assigned to seats on the airplane while maintaining social distancing guidelines, which shares the objective of RCV but makes social distancing a hard constraint. The difference between model 2 and RCV is similar to the difference between model 1 and VPR: model 2 is constrained by Euclidean distance measurements between seats, and RCV is constrained by total virus transmission risk probabilities. If VPR and RCV are given risk transmission models based solely on distance, then the solutions are similar to model 1

and model 2, but VPR and RCV allow for other risk models that may be more accurate, such as the coughing risk model based on both distance and direction described in Section 4 or the potential ECS-specific models in Section 6.

3. Modeling

We formally introduce the two problems: VPR and RCV. Let $G = (V, E)$ be an undirected graph with edge costs $c : E \to \mathbb{R}^+$ representing transmission risks.

3.1. VPR

Consider a target number of vertices N such that $0 \le N \le |V|$. The vertex packing risk minimization problem is to find $P \subseteq V$ such that $|P| = N$ and the sum of the edge costs (total risk) in the subgraph induced by P is minimized. Using vertex indicator variables x_v, where $x_v = 1$ if vertex v is included in the solution and 0 otherwise, and edge indicator variables z_{uv}, where $z_{uv} = 1$ if both vertices u and v are included in the solution and an edge exists between u and v, and 0 otherwise, we obtain the following model:

$$\begin{aligned}
\text{minimize} \quad & \sum_{uv \in E} c_{uv} z_{uv} \\
\text{subject to} \quad & \sum_{v \in V} x_v = N, \\
& x_u + x_v - 1 \le z_{uv} \quad \text{for all} \quad uv \in E, \\
& x_v \in \{0,1\} \quad \text{for all} \quad v \in V, \\
& z_{uv} \in \{0,1\} \quad \text{for all} \quad uv \in E.
\end{aligned}$$

In the context of airplane seating assignments, VPR has a fixed N number of passengers to seat, and the solution is a seating configuration with the least risk of spreading a transmissible disease between passengers.

VPR and GIS are similar problems because both extend the independent set problem in different ways. The GIS linear model can be extended to solve VPR problems by setting vertex weights $w_v = 0$ for all $v \in V$ and adding the constraint $\sum_{v \in V} x_v = N$.

We show that VPR is NP-hard in the general case using a reduction from vertex packing.

Theorem 1. *VPR is NP-hard.*

Proof. The proof is by reduction from the vertex packing problem, a known NP-hard problem. Let $G = (V, E)$ be an instance of the vertex packing problem. Construct graph G' from G by adding unit edge costs. The maximum cardinality of an independent set in G can be found by solving VPR repeatedly within a binary search on N, the required size of the vertex set.

Formally, initialize a lower bound $\ell = 0$ and an upper bound $u = |V|$. Solve VPR on G' for $N = \lfloor (u - \ell)/2 \rfloor$ seats to obtain $S \subseteq V$, a vertex set of cardinality N with minimal risk. If S has risk zero, and hence S is an independent set, we update ℓ to N and continue the binary search. Otherwise (i.e., S has positive risk), we update u to N and continue the binary search. After updating either u or ℓ, we set $N = \lfloor (u - \ell)/2 \rfloor$.

The binary search ends when $\ell \ge u$, which occurs after $O(\log_2 |V|)$ iterations. After the binary search ends, ℓ is the maximum cardinality of a vertex set with zero risk for the constructed VPR instance. By construction, ℓ is also the maximum cardinality of an independent set in G, the given vertex packing problem instance. Hence if a polynomial time algorithm exists for VPR, then a polynomial time algorithm exists for the vertex packing problem. ■

If VPR is used to solve airplane seating problems, then complications may arise such as an extra passenger showing up late to boarding. In those cases, it is useful if the seating solution provided by VPR for the first N passengers is a subset of the solution for $N + 1$ passengers, such that the passengers already seated would not be required to move in the new minimum risk solution. Unfortunately, this is not always possible.

Proposition 1. *An optimal solution to an instance of VPR of size N is not necessarily a subset of an optimal solution of size* $N + 1$.

Proof. Consider the VPR instance where $G = P_7$ (the path on seven vertices, as shown in Figure 1(a)); $N = 3$; and the cost function $c : E \to \mathbb{R}^+$ is given by $c_{uv} = 1$ if u and v are exactly two edges (one empty seat) apart, $c_{uv} = 5$ if u and v are adjacent, and $c_{uv} = 0$ otherwise. The only optimal solution is to fill the first, fourth, and seventh seats, as shown in Figure 1(b), for a total risk of zero units. Increasing the number of occupied seats to $N + 1 = 4$, the only optimal solution is to fill every other seat, as shown in Figure 1(c), for a total risk of three units. But if the solution for $N = 4$ must fill the seats used by the optimal solution for $N = 3$, then the least possible risk is six units, obtained by filling any one of the four empty seats in Figure 1(b). Hence an optimal solution for $N = 3$ is not necessarily a subset of an optimal solution for $N = 4$. ■

3.2. RCV

Consider a maximum acceptable total risk, R. The risk-constrained vertex packing problem is to find a set of vertices $P \subseteq V$ of maximum cardinality such that the sum of the edge costs in the subgraph induced by P is at most R.

Using vertex indicator variables x_v, where $x_v = 1$ if vertex v is included in the solution and 0 otherwise,

Figure 1. Graphic Demonstration of the Potential Necessity of Repacking as N Increases

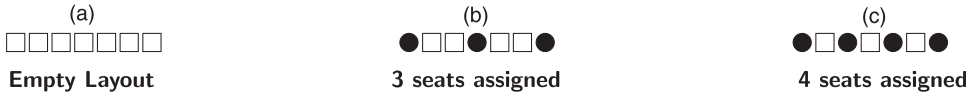

Notes. White squares represent empty seats. Black circles represent filled seats.

and edge indicator variables z_{uv}, where $z_{uv} = 1$ if both vertices u and v are included in the solution, and an edge exists between u and v and 0 otherwise, we obtain the following model:

$$\begin{aligned}
&\text{maximize} \sum_{v\in V} x_v \\
&\text{subject to} \sum_{uv\in E} c_{uv} z_{uv} \le R, \\
&\qquad x_u + x_v - 1 \le z_{uv} \quad \text{for all} \quad uv \in E, \\
&\qquad x_v \in \{0,1\} \quad \text{for all} \quad v \in V, \\
&\qquad z_{uv} \in \{0,1\} \quad \text{for all} \quad uv \in E.
\end{aligned}$$

In the context of airplane seating assignments, RCV has maximum risk R of spreading transmissible diseases, and the solution finds as many passengers as possible to seat without exceeding the given risk.

GVP-k and RCV have a similarity much like GIS and VPR. GVP-k can solve RCV problems by setting k to the maximum allowable risk from an RCV instance and adding edge costs as coefficients on each edge decision variable z_{uv}, making the first constraint $\sum_{uv\in E} c_{uv} z_{uv} \le k$. However, Sherali and Smith (2006) only considered k to be integral instead of real valued, and hence their approach to solving GVP-k cannot solve all RCV instances using this construction.

We show that RCV is an NP-hard problem in the general case using a reduction from vertex packing.

Theorem 2. *RCV is NP-hard.*

Proof. The proof is by reduction from the vertex packing problem. Let $G = (V, E)$ be an instance of the vertex packing problem. Construct G' from G by adding unit edge costs. Solve RCV on G' using $R = 0$. An optimal solution of the RCV instance is an independent set (because $R = 0$ and $c_e = 1$ for all $e \in E$); therefore the RCV solution corresponds to an optimal solution of the given vertex packing problem instance. The reduction is clearly polynomial, and hence RCV is NP-hard. ■

4. Airplane Transmission Risk Modeling

VPR and RCV are abstract models. Our goal is to solve the more practical airplane seating assignment problem. Given the high mortality rate attributable to COVID-19 in 2020, we are most interested in minimizing the risk of transmitting SARS-CoV-2. However, there are no papers to date that estimate the transmission risks for SARS-CoV-2 in an aircraft environment. Several papers have studied the transmission risks for influenza in aircraft, and hence we will use the influenza risks to build our models until SARS-CoV-2 risks can be determined.

Influenza and SARS-CoV-2 are transmitted by a variety of methods. Contact transmission involves direct physical contact between two people, during which respiratory secretions pass from one person to the other. Droplet transmission occurs when droplets greater than 5 μm in diameter released during an exhalation (e.g., coughing, sneezing, and talking) land in the mouth, nose, or eyes of a susceptible person. Airborne transmission occurs when droplet nuclei less than 5 μm in size are generated and then inhaled by another person, as the smaller droplet nuclei are light enough to remain airborne instead of falling to the ground. Fomite transmission occurs when secretions or droplets land on an object and contaminate it and then the object is picked up by another person, causing an indirect contact transmission. Other modes of potential transmission, such as blood or animal contact, are unlikely to be significant factors on an airplane and are therefore excluded from aircraft cabin transmission risk models.

Wan et al. (2009) provided simulated transmission risk values of influenza spread via airborne and droplet transmission based on an infection model from Sze et al. (2008). Their simulation and validation experiment used a small cabin with 12 seats in a 3-row × 4-column configuration, with the infected patient located in the rearmost row and leftmost column. The authors reported that the inhalation risk was highest for the passenger directly in front of the index patient (58%), approximately an order of magnitude less for the passengers diagonally in front of (7%) or in the same row as (3%–4%) the index patient, and smaller risks (less than 2%) for all other passengers (Wan et al. 2009, table 6, row "200 L/s").

Zhang and Li (2012) simulated respiratory droplets in a high-speed rail cabin. The seating configuration of four seats per row with a center aisle is similar to many airplanes, and their case 2 ECS was also similar to the ECS configuration used in Wan et al. (2009), with no throughflow of air, ceiling inlets, and floor exhaust vents. In that configuration, they found that the majority of droplet dispersion was limited to one row forward and backward (Zhang and Li 2012, figures 9 and 10). The authors did not use any infection modeling to assign risks of disease transmission.

Wan et al. (2009) and Zhang and Li (2012) assumed that the passengers remained in their seats. Hertzberg et al. (2018) studied the behavior and movement of passengers and crew on 10 transcontinental flights in order to develop a network model of infection transmission. They found that passengers in aisle seats were twice as likely as those in window seats (80% versus 43%) to get up and move about the cabin at least once, with the majority of movement being to use the lavatory or check an overhead bin. Passengers sitting in window seats were also less likely to have close proximity contact with moving passengers because of the distance from the aisle. Their model simulated direct influenza transmission for an index passenger located in an aisle seat in the middle of the airplane. The simulation modeled that passengers seated within one row forward or backward and two columns left or right of the infectious patient (11 nearest neighbors) had the highest probability of infection (greater than 80%). Crew members walking the aisles were the next most likely to be infected (5%–20%). Every other passenger had a very small probability of infection (less than 3%) (Hertzberg et al. 2018, figure 3). Their model assumed a flat infection rate of 0.018 per minute of contact, with no coughing or sneezing, and the median contact time between the infectious patient and passengers seated more than one meter away was only 24 seconds.

None of these studies consider the use of face masks, which disrupt the trajectory of aerosol droplets during a cough. Tang et al. (2009) suggested that turbulent jets of aerosols still escape from the mask perimeter, both vertically and laterally. Grinshpun et al. (2009) studied the performance of N95 respirators and surgical face masks during normal breathing and found the N95 to reduce particle penetration by 94% and the surgical mask to reduce penetration by 50%, including penetration from both leakage around and passing through the filter. Nir-Paz et al. (2020) suggested that face masks are effective in limiting transmission of SARS-CoV-2 aboard aircraft. In lieu of more quantitative experimentation with face masks, the relative risk of transmission to each of the nearby seats is assumed to decrease uniformly with the use of a mask. However, future experimentation could lead to mask-based risk models that reduce the longitudinal (forward-facing) risks and increase lateral (side-to-side) risks, which would lead to different optimal seating strategies than those presented in this paper.

We distill these assorted risk models into two simplified models, coughing and noncoughing, for use as inputs to the VPR and RCV problems. In both models we combine transmission risks to create undirected edge costs that are the sum of the pair of transmission risks. Given two passengers, u and v, then the edge cost c_{uv} of a risk model is the risk of u infecting v plus the risk of v infecting u. It is not required to use simplified or generic risk models; if sufficient data are available through either modeling or experimentation, then every pair of seats on the airplane can be assigned an individualized risk value.

4.1. Coughing

The coughing model represents the risk of a stationary patient who coughs. The model is extrapolated from the 200 liters per second results in table 6 of Wan et al. (2009) in order to accommodate an infectious patient sitting in any seat on an airplane instead of only the rear left corner. The ECS system is assumed to cause lateral airflow, which means the infectious droplets are more likely to spread to further columns than to further rows. Because of the force with which coughing spreads aerosol droplets, the most dangerous seat is directly in front of an infectious patient. In the coughing model, $c : E \to \mathbb{R}^+$ is given by

$$c_{uv} = \begin{cases} 0.58 & \text{if } u \text{ is directly behind } v \text{ or vice versa,} \\ 0.07 & \text{if } u \text{ and } v \text{ are within one row and one column (and not directly behind),} \\ 0.04 & \text{if } u \text{ and } v \text{ are within one row and between two and four columns,} \\ 0 & \text{otherwise.} \end{cases}$$

We can compare the coughing model, based on influenza data, to a case study of a coughing SARS-CoV-2-positive passenger. In figure 1 of Khanh et al. (2020), the index passenger in business class likely caused transmission to 11 of the 12 passengers seated within two rows and four columns of her seat (all within two meters). An additional passenger in the same row and five columns away also tested positive and was a likely transmission from the index passenger. This comparison suggests that the coughing model may be underestimating the SARS-CoV-2 risks for very long flights (10 hours in the case study) or that some passengers may be more infectious than others.

4.2. Noncoughing

The noncoughing model represents the risk of a stationary patient who is not coughing, based on figure 3 of Hertzberg et al. (2018). In this model, anyone near an infectious patient is likely to become infected. To prevent this from becoming a complete graph where every passenger is at risk from every other passenger, we limited the distance to only adjacent rows based on the results from Zhang and Li (2012), with all other risks rounded down to 0. In the noncoughing model, $c : E \to \mathbb{R}^+$ is given by

$$c_{uv} = \begin{cases} 0.9 & \text{if } u \text{ and } v \text{ are within one row and two columns,} \\ 0 & \text{otherwise.} \end{cases}$$

Hertzberg et al. (2018) only reported a range of 0.8–1.0 for the risks in their model for the passengers within one row and two columns; therefore, we used the middle of their given range for passengers near the index patient. Comparing the noncoughing risk model to the COVID-19 case study from Figure 1 of Khanh et al. (2020), all four (100%) of the passengers within one row and two columns of the index patient became infected with SARS-CoV-2, consistent with the 90% infection rate predicted by the noncoughing model among patients not wearing masks. Eight other nearby passengers became infected, but the noncoughing model would predict a 0% infection rate for them, suggesting that this model also underestimates the risks for a very long (10-hour) flight.

An aisle is treated as an empty column in both the coughing and noncoughing risk models.

4.3. Risk Score

The risk score calculated by both VPR and RCV is the cumulative risk score. The cumulative risk score is the sum of every potential risk of transmission between each pair of seats, and it assumes that every passenger can potentially infect every other passenger.

In both models the infectious passengers are assumed to be seated far enough away from each other that there is no overlap in transmission risks. If this assumption does not hold, then a cumulative risk score that sums the transmission risk of every pair of seats may overestimate the actual risks. For example, if 10 passengers are already infected, but they all sit next to each other, then the risk score would overestimate the risks by assuming they would transmit the disease to each other and by assuming that other nearby passengers could be infected more than once. However, if there is only one infectious passenger, or the multiple infectious passengers are far enough apart that they do not have any overlapping risks with nearby passengers, then the cumulative risk score correlates with the expected number of infections.

Given a few assumptions, the cumulative risk score can be converted into a normalized risk score. First, assume exactly one passenger is infectious. Second, assume the infectious passenger is equally likely to sit in any seat on the aircraft. Third, assume each edge cost/risk is the infection transmission probability for that flight. The normalized risk score is therefore the cumulative risk score divided by the number of passengers on the aircraft. The normalized risk score captures the average risk of any individual seat on the aircraft, which may be useful for a passenger trying to choose between different flights. The normalized risk score also represents the expected number of new infections from the flight given a single infected passenger.

5. Computational Results

Solutions can be precomputed for the airplane seating assignment problem; it is not necessary to solve them in real time. For a given aircraft and transmission risk model instance X, the number of possible input values of N to the VPR on instance X is finite and equal to the number of seats on the aircraft, while the input to RCV is a continuous value R between zero and infinity. Given an input constraint N, let R' be the minimized risk value from the VPR instance solved with input N. If RCV on instance X is given R' as the input constraint for R, then the RCV instance will output a seat configuration with N seats. Hence, solving all possible input values for an instance of VPR also solves every possible output value of RCV on that same instance, and is sufficient to precompute solutions before the actual number of passengers is known.

This section investigates VPR and RCV problem tractability when applied to a variety of airplane input graphs, and examines VPR results when applied to a Boeing 717-200. We built a 2D structure for each airplane, with each seat placed in a row and column corresponding to its physical location in order to maintain the same approximate distance between seats as would occur on the airplane, using the seat maps provided at https://www.delta.com/us/en/aircraft/overview.

We used CPLEX 12.10 to solve each model. All of the computation was performed on a workstation computer using an AMD 9 3900X 12 core/24 thread CPU running at 3.8 GHz with 128 GB of DDR4 2666 MHz RAM, and reported times are the CPU times output by CPLEX. All of the experiments were set to terminate at an optimal solution, 6 hours of CPU time, or 100 GB of memory, whichever comes first.

In order to determine how tractable VPR and RCV problems are in practice, we ran a series of tests and report the results in Table 1. For the VPR tests, one run was performed for each possible number of seats for each plane, one passenger up to the full capacity of the airplane, with results reported as the number of runs solved optimally. VPR C is the vertex packing risk minimization problem with edge weights generated by the coughing model. VPR NC uses the noncoughing risk model. The RCV tests are run with 0, 100, 1,000, and 10,000 as the maximum risk inputs. RCV C and NC are the risk constrained vertex packing problem with the coughing and noncoughing risk models, respectively.

Problem instances for smaller planes, consisting of 150 seats or less, were solved to optimality under the CPLEX resource limits for VPR with both risk models. Some larger planes, such as the A350-900, have bulkheads or restrooms that section the cabin into separate areas. This creates an input graph of disconnected subgraphs, with no shared risk, reducing the difficulty of solving the large, sectioned planes.

Table 1. Airplanes Tested—Number of Optimal Solutions Discovered

Make	Type	Seats	VPR C	VPR NC	RCV C	RCV NC
Airbus	A220-100	109	109	109	4	4
	A319-100	132	132	132	4	4
	A320-200	157	144	151	4	4
	A321-200	191	178	183	3	4
	A330-200	234	209	234	3	4
	A330-300	293	253	293	3	4
	A330-900NEO	281	253	281	3	4
	A350-900	306	254	291	3	3
Boeing	717-200	110	110	110	4	4
	737-700	124	124	124	4	4
	737-800	160	147	156	4	4
	737-900ER	180	167	175	4	4
	757-300 (75D)	199	184	190	4	4
	767-300ER (76T)	211	190	207	4	4
	777-200ER	296	246	280	3	3
	777-200LR	288	241	269	3	2
Bombardier	CRJ-200	50	50	50	4	4
	CRJ-700	69	69	69	4	4
	CRJ-900 (RJ8/CM8)	70	70	70	4	4
	CRJ-900	76	76	76	4	4
Embraer	ERJ-170	69	69	69	4	4
	ERJ-175	76	76	76	4	4
McDonnell Douglas	MD-88	149	149	149	4	4
	MD-90	163	162	161	4	4

Notes. Each solution ran until it found optimal, reached the CPU limit (6 hours), or reached the memory limit (100 GB). C, coughing risk model; NC, noncoughing risk model. VPR performed one test for each possible number of passengers from 1 to the number of seats on each model; RCV performed four tests.

Table 2 looks at the Airbus A320-200 as an example of an airplane that could not be completely solved optimally in order to examine the quality of nonoptimal solutions. The 29-passenger test was solved optimally in 33 CPU seconds, but after 6 hours CPLEX was not able to determine a best bound for the 30-passenger test. No best bound means that CPLEX was not able to eliminate the possibility of a zero risk solution and hence the reported relative gap is 100%. The other nonoptimal passenger tests, 31–42 passengers, ranged from a 65% to a 7% relative optimality gap between the best integer solution discovered and the best-known bound after 6 hours of CPU time. A 0% optimality gap would mean the solution is definitely optimal.

5.1. Coughing Risk Model Results

Figures 2 and 3 cover the minimum normalized risks and marginal normalized risks for a single airplane, the Boeing 717-200, when solved using the coughing risk model. Normalized risk is the same as the expected number of new infections given a single infected passenger on the airplane. Marginal normalized risk is the change of the normalized risk for one more passenger added to the plane, with all passengers are allowed to move to a new optimal configuration. Marginal normalized risk for N seats is calculated as the change in normalized risk between $N-1$ and N seats, and hence the sum of the marginal normalized risk from 1 to N in Figure 3 is the same value as the normalized risk for N in Figure 2. The repetitive nature of the airplane's seating layout creates phases, highlighted by the increases in marginal risk. The boundary points where marginal risk dramatically increases are shown in Figure 4. There exists a

Table 2. Airbus A320-200 Solved Using VPR with Coughing Risk Model

Make	Type	Seats	Passengers	Relative gap (%)
Airbus	A320-200	157	30	100.00
			31	65.08
			32	38.99
			33	20.00
			34	20.16
			35	32.38
			36	14.20
			37	27.62
			38	24.76
			39	28.14
			40	22.05
			41	26.30
			42	7.00

Notes. All solutions below 30 seats or above 42 seats were solved optimally. The relative gap is the difference between the best bound and best integer solution divided by the best integer solution discovered by CPLEX at the time of termination. All tests in the table were terminated upon reaching 6 hours of CPU time.

Figure 2. Normalized Risk Values for Each Possible Passenger Count in a Boeing 717-200 with the Coughing Risk Model

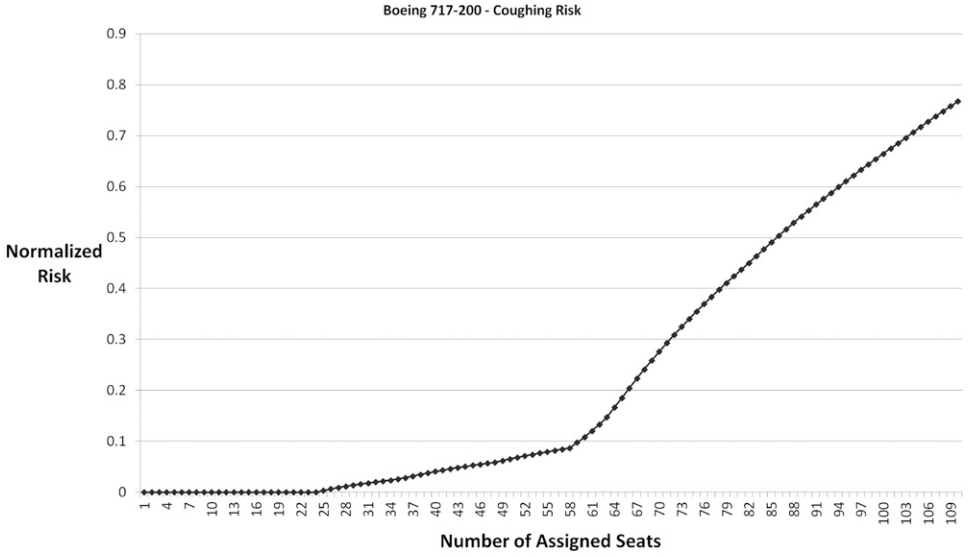

zero-risk (i.e., independent set) solution from 0 to 24 passengers with a repeating pattern of filling window seats. At 58 seats, every other row has been filled, and any configuration of 59 passengers must include at least one passenger in front of or behind another passenger, causing a large increase in marginal risk.

Different input values of N take significantly different amounts of time to solve. The extreme values are the simplest to solve from a combinatorial perspective. For example, on the VPR problem, if there are zero passengers or zero empty seats, then that configuration is optimal as no other configurations are possible. The values in the middle are more difficult to solve but are mostly tractable on graphs of the size of airplanes. The largest airplanes have approximately 300 vertices, but the largest airplanes are also broken up into sections spaced far enough apart to create disconnected subgraphs.

Figure 3. Marginal Normalized Risk Values (i.e., Normalized Risk Added) for Each Possible Passenger Count in a Boeing 717-200 with the Coughing Risk Model

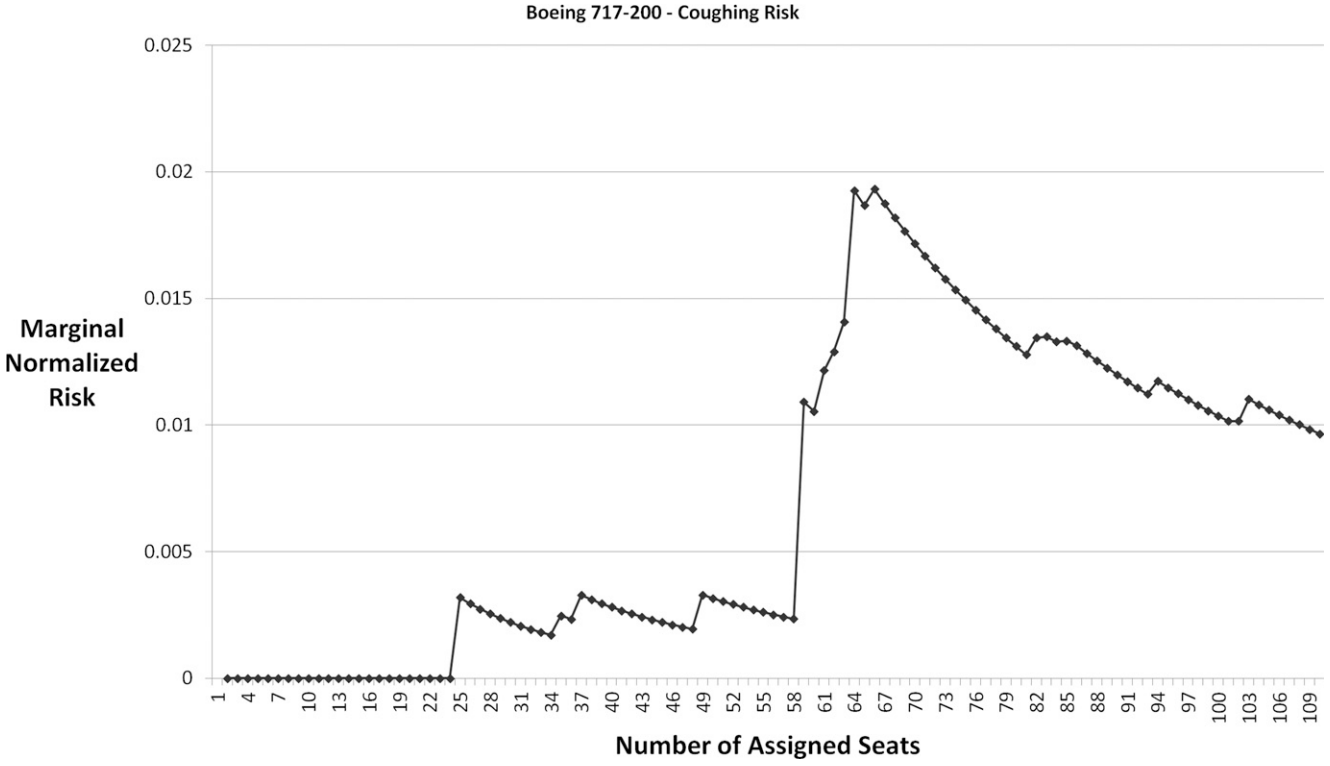

Figure 4. Boeing 717-200 Solved Using VPR with the Coughing Risk Model

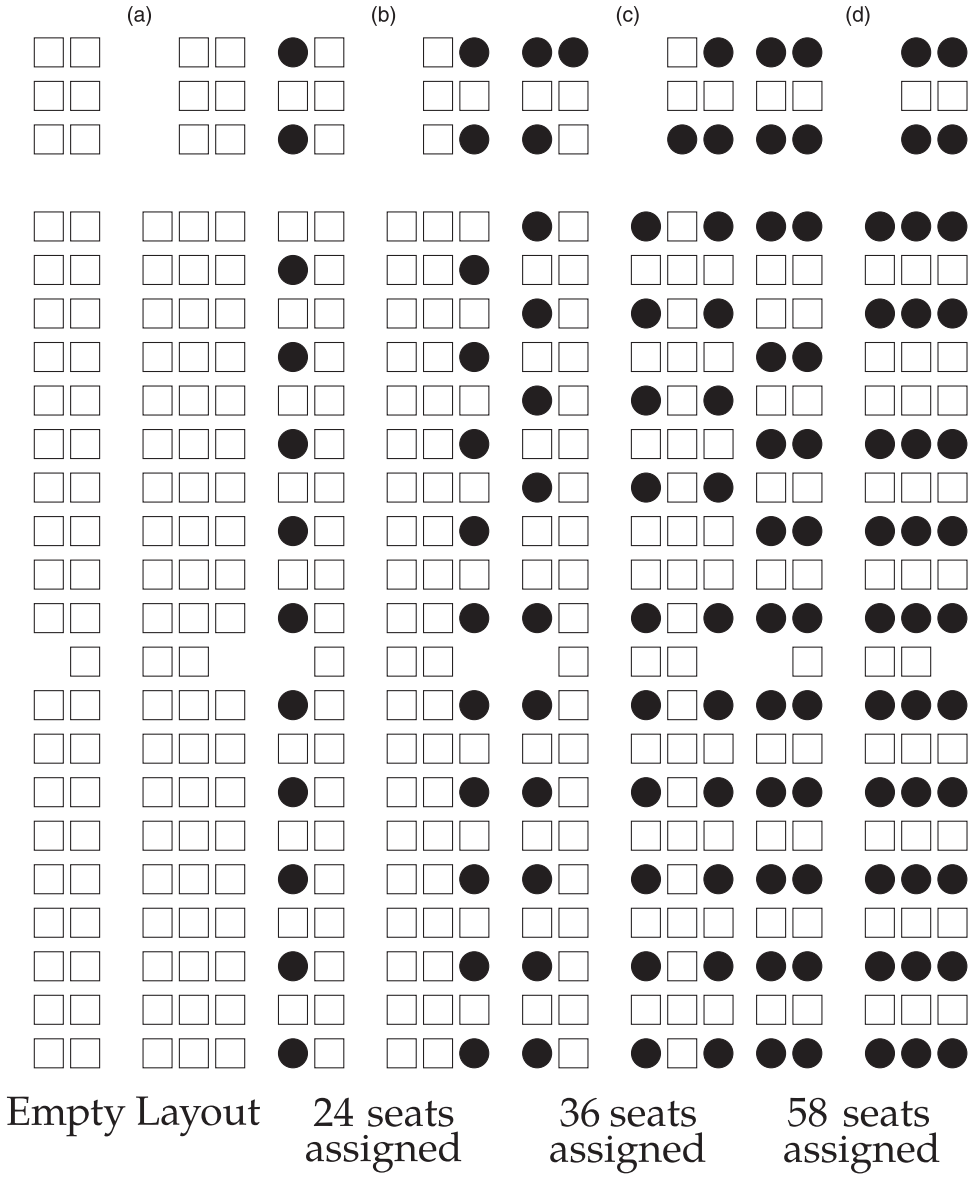

The Boeing 717-200 is a smaller aircraft at 110 seats, but it is illustrative of the patterns of solving VPR problems. The CPU time results for the Boeing 717-200 with the coughing risk model are reported in Figure 5. Any instance where an independent set can be identified (i.e., 1–24 passengers) is solved in less than 0.1 CPU seconds. Problems consisting of seating 25–32 passengers are the most difficult, taking 69–185 CPU seconds to solve. In the worst case, the problem takes 3 minutes of CPU time to solve, but given a 24-thread desktop CPU, the wall clock time was under 10 seconds.

5.2. Noncoughing Risk Model Results

The noncoughing model differs from the coughing model in that simply being near an infected passenger is considered high risk, with no differentiation between relative positioning. The risk is the same regardless of whether the infected passenger is beside or behind other passengers.

Figures 6 and 7 show the normalized risk and marginal normalized risk for a Boeing 717-200 using the noncoughing risk model. As in the coughing model case, marginal normalized risk for N seats is the difference in normalized risk between $N - 1$ and N seats. Figure 7 has one notable feature that distinguishes it from the coughing version: the noncoughing marginal risk has a repeating decrease, then increase in value every second passenger from 77 to 88 seats assigned. This is caused by seating rearrangements that occur when assigning the odd-numbered passenger, as described in Proposition 1. Before each pair of odd and

Figure 5. CPU Time to Solve for Each Possible Passenger Count in a Boeing 717-200 with the Coughing Risk Model

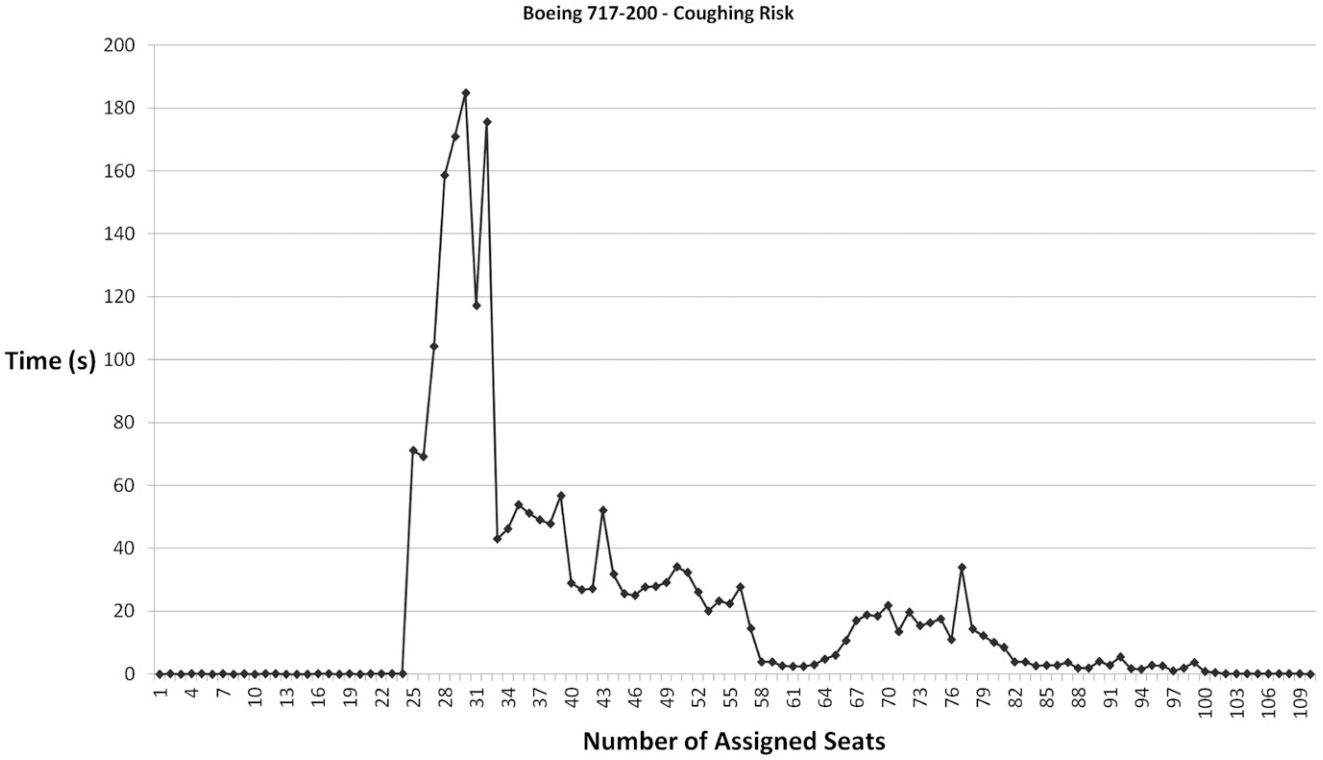

even passengers is placed in that 76- to 90-seat range, one existing passenger is moved from sitting within one row and two columns of four passengers to a different nearby seat that is within range of five passengers. Both the odd and even passengers are each then placed close to five existing passengers, so that the moved passenger and both added passengers are near five other passengers for 15 cumulative (not normalized) risk edges of 0.9 each. If a passenger was not moved, then the unmoved passenger is near four other passengers, but both added passengers must be near six passengers each, for a total of 16 risk edges of 0.9 each. The data do not show the moved passenger as a separate entry because the moved passenger is part of the new solution, and hence the first (odd) passenger of each pair added has a marginal cumulative risk of 5.4, from six edges, whereas the second (even) passenger of each pair has a lower

Figure 6. Normalized Risk Values for Each Possible Passenger Count in a Boeing 717-200 with the Noncoughing Risk Model

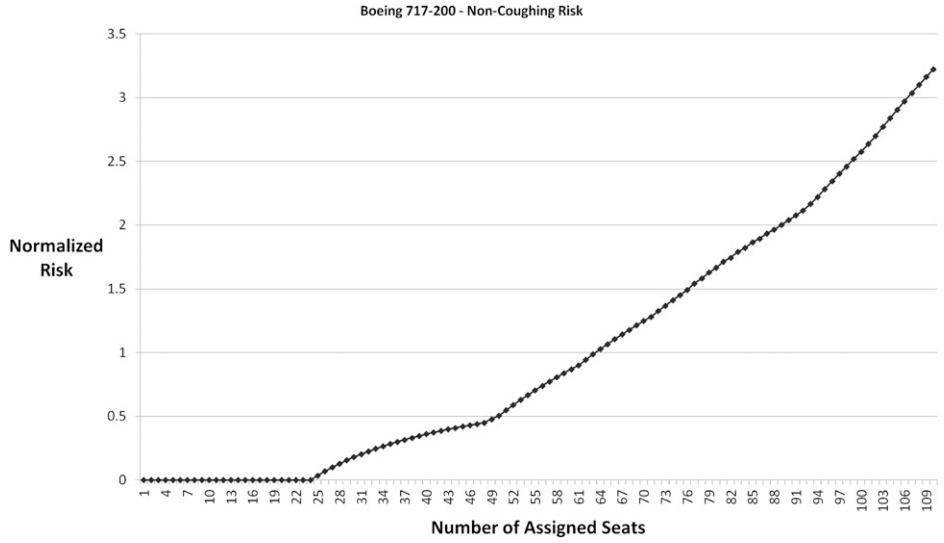

Figure 7. Marginal Normalized Risk Values (i.e., Normalized Risk Added) for Each Possible Passenger Count in a Boeing 717-200 with the Noncoughing Risk Model

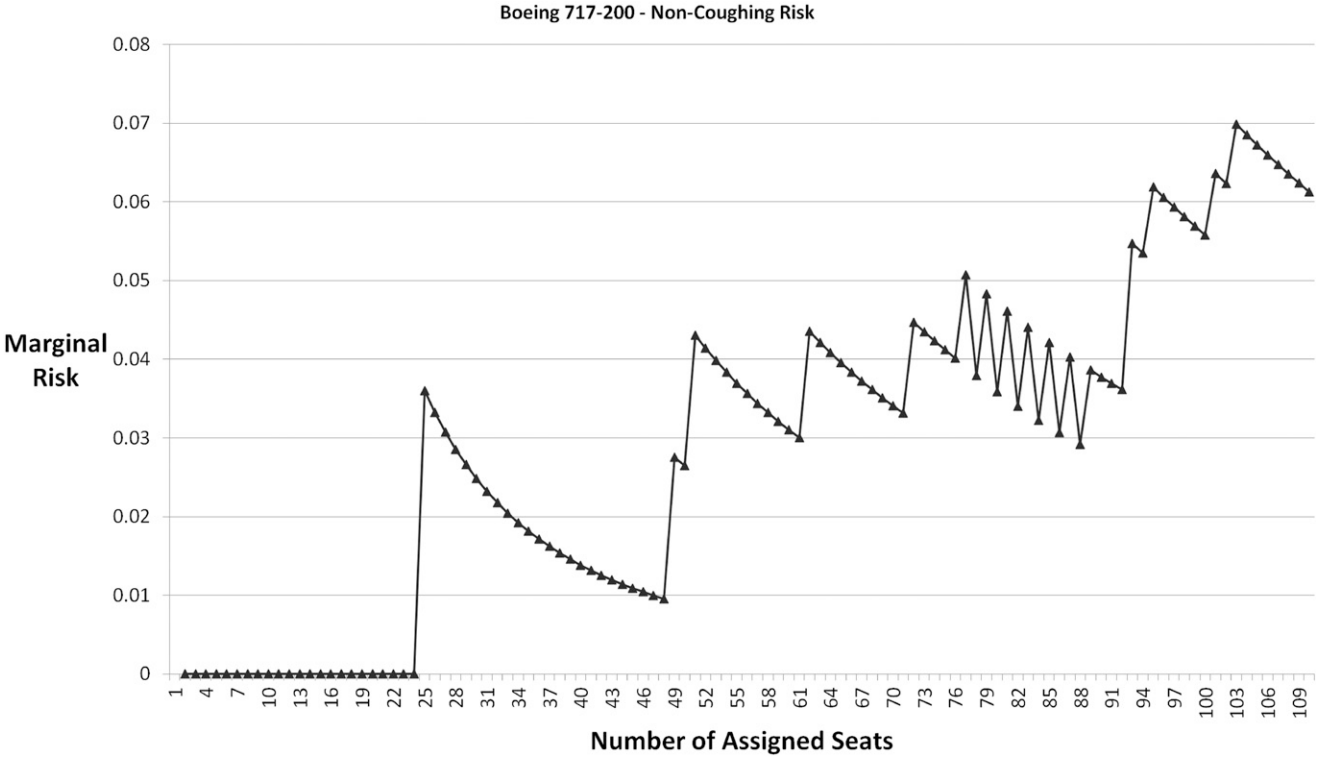

marginal cumulative risk of 4.5, from five edges. Each pair has the same cumulative risk, so normalization causes the downward trend as the number of passengers increases.

Figure 8 shows the seating arrangements at several of the major boundary points in marginal risk. The 61-seat and 82-seat subfigures show that the noncoughing model is more likely to place passengers in the same column in different rows, instead of filling the same row and leaving alternating rows empty with the coughing model.

Figure 9 shows the time taken for VPR to solve each possible number of passengers with the noncoughing model. All the passenger counts were able to be solved optimally, with the most difficult problems again being the least numbers of passengers who cannot form an independent set.

Figure 10 shows a direct comparison between the coughing and noncoughing models at both 55 and 85 seats assigned. The coughing model favors leaving alternating rows empty because it assigns a higher risk to passengers who sit in front of another passenger. The noncoughing model favors leaving the aisle seat empty because it assigns the same risk to passengers who sit side by side and who sit one seat apart, and the aisle seat is close enough to the filled seats to create risk from the other side.

One existing solution adopted by some airlines to mitigate risk is to block the middle seats. Reducing the number of passengers on the airplane will either decrease risk or make no change, as no passenger can create negative risk. However, the minimum risk configuration under both the coughing and noncoughing models may require seating a passenger in the middle seat of a row.

Using the Boeing 717-200 and the noncoughing risk model as an example, Figure 11 compares the risks of blocking middle seats to not blocking (i.e., using all seats), with seating arrangements in both cases provided by VPR. From 0 to 35 passengers, there is no difference in risk. The passengers can distance themselves in ways that reduce their risk without needing a middle seat, as shown in Figure 12(a). However, from 36 to 65 passengers, using all seats has a lower risk than blocking the middle seats. At 65 passengers, the plane is entirely full, except for the blocked middle seats.

Figure 13 shows the normalized optimal risk of the Boeing 717-200 with the noncoughing risk model compared with an $N + 1$ risk, where the $N + 1$ risk is calculated by assigning one passenger at a time to a minimum risk position without allowing any of the previous N passengers to reseat themselves. This is a test of how much risk may be added when not reseating passengers in accordance with Proposition 1.

Figure 8. Graphic Demonstration of Seating Arrangements Produced by VPR with the Noncoughing Risk Model on a Boeing 717-200

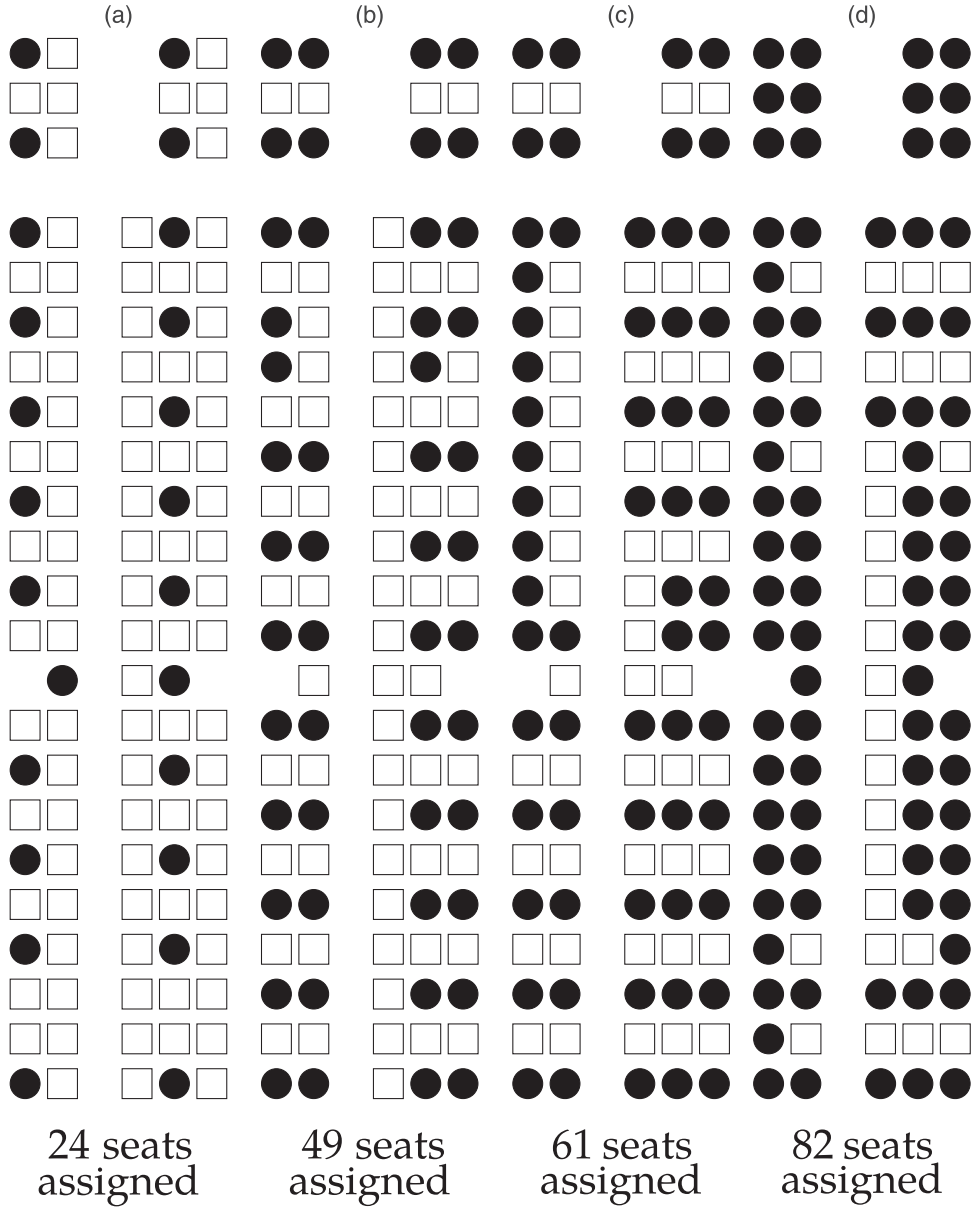

Multiple optimum configurations may exist for each value of N passengers, and this test uses the configuration returned by CPLEX, but other equally optimal configurations of N passengers may result in lower or higher risk values for $N + 1$. Figure 14 shows the $N + 1$ line divided by the optimum risk, in order to show how much higher the $N + 1$ risk is relative to optimum. The $N + 1$ risk is equal to the optimum as long as the number of passengers is at 38 passengers or fewer, with a large spike in risk peaking at 48 passengers, with 142% relative risk. There are only a few possible configurations when the plane is mostly empty or almost full, and hence, the $N + 1$ risk is equal to the minimum risk in those ranges.

Figure 15 shows the effect of using the wrong risk model. The crossover risk value is calculated by finding an optimal seating arrangement based on the noncoughing risk model and then using that seating arrangement to find the risk under the coughing risk model. The coughing line shows an optimal seating arrangement based on the coughing risk model. Normalized risk sometimes decreases with an increase in assigned seats because there may be different configurations with the same optimum risk for the noncoughing model but different risks for the coughing risk model. There is no particular tie-breaking being applied for the noncoughing model, so sometimes the extra person causes a different

Figure 9. CPU Time to Solve for Each Possible Passenger Count in a Boeing 717-200 with the Noncoughing Risk Model

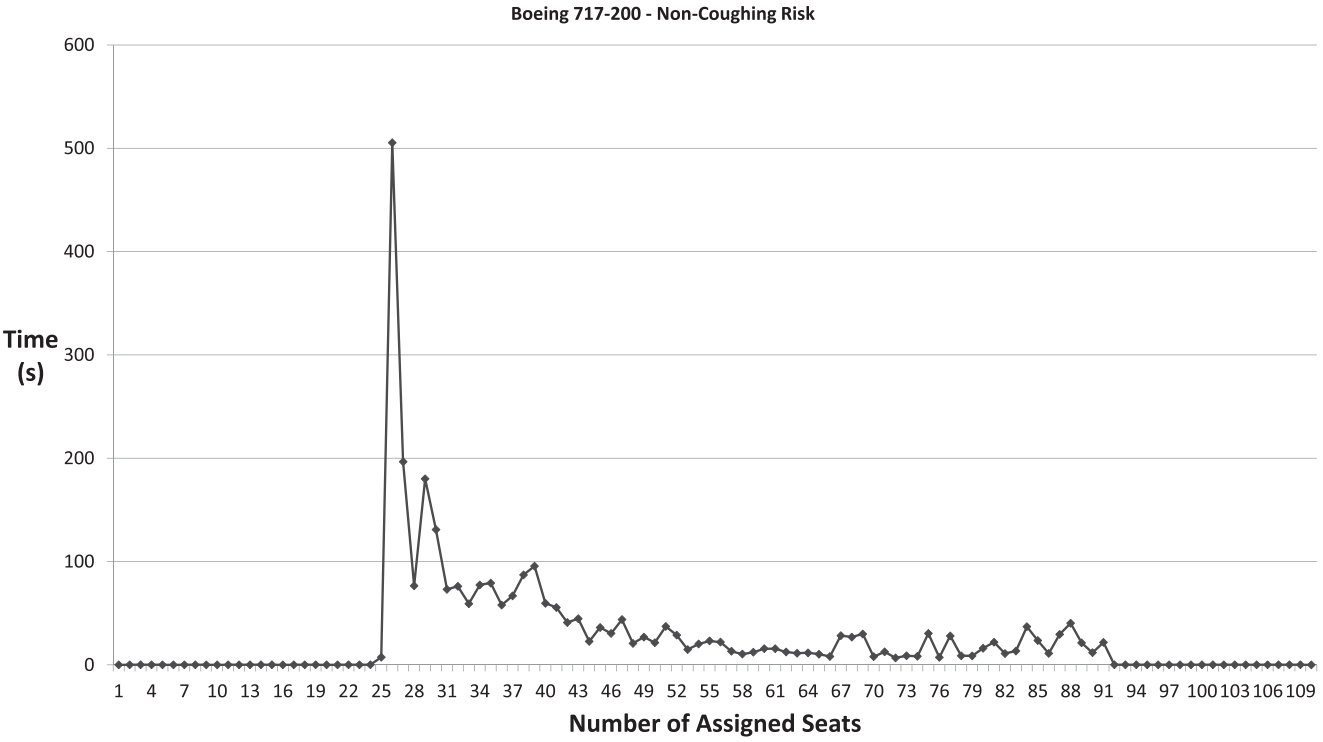

seating arrangement that is more favorable for the coughing seating risk.

6. Conclusions

Public health demands that reasonable precautions be taken to reduce the transmission of SARS-CoV-2 between airplane passengers. We introduce the airline seating assignment problem ASAP and develop the models VPR (vertex packing risk minimization) and RCV (risk-constrained vertex packing) to solve it. Although we focus on solving ASAP, VPR and RCV problems are tools that can be used to solve seating

Figure 10. Comparison Between Coughing and Noncoughing Model Results

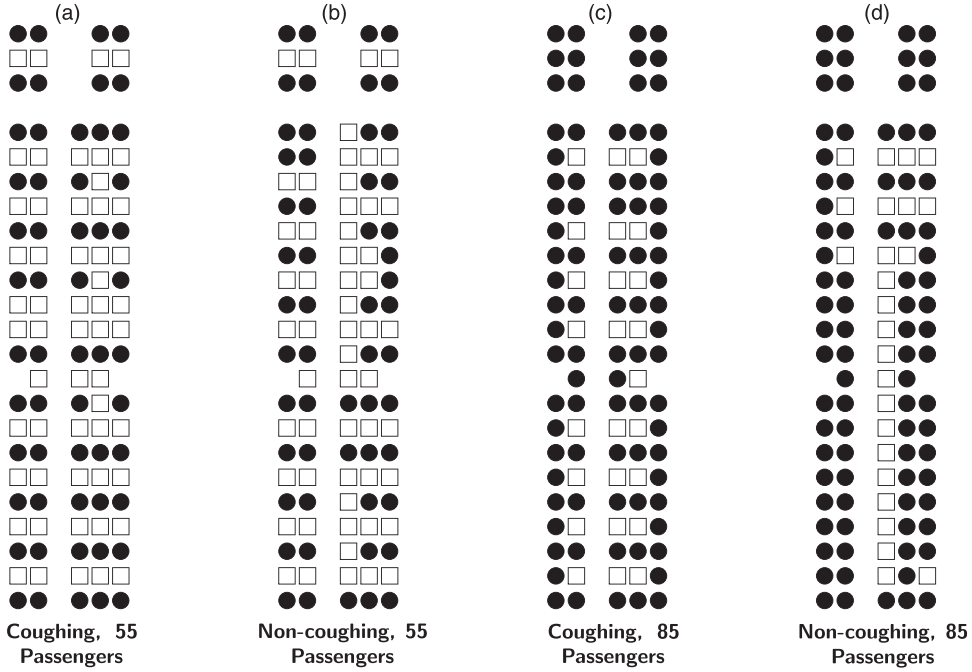

Figure 11. Boeing 717-200 Normalized Risk Comparison Between Using No Middle Seats and Using All Possible Seats, with the Noncoughing Risk Model

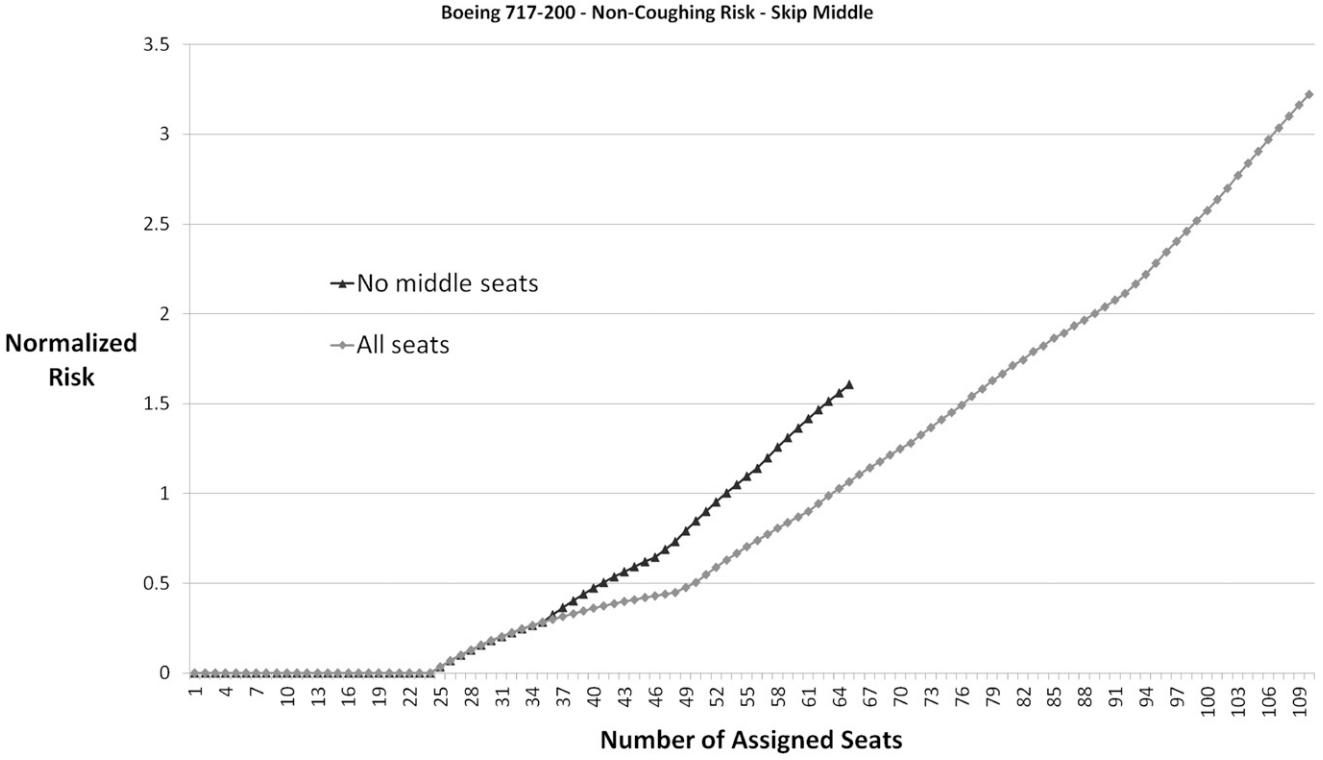

assignments in a wide variety of real-world situations, such as theaters or stadiums. We demonstrate that a standard commercial solver is capable of optimally solving most aircraft instances quickly and finds good feasible solutions for the remainder. In the future, faster algorithms could be developed to solve VPR and RCV by designing problem-specific algorithms instead of using standard commercial solvers.

Figure 12. Graphic Comparison of Seating Arrangements Produced by Strategies of Blocking Middle Seats and Using All Seats with VPR and the Noncoughing Risk Model

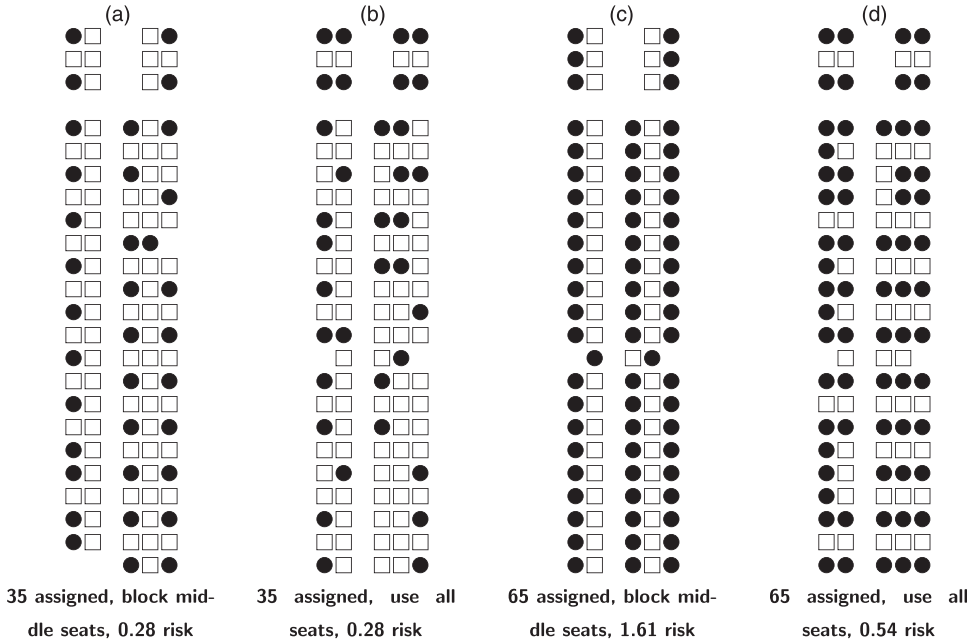

Figure 13. *N* + 1-Normalized Risk Compared with the Optimal Normalized Risk for Each Number of Passengers, Using the Noncoughing Model

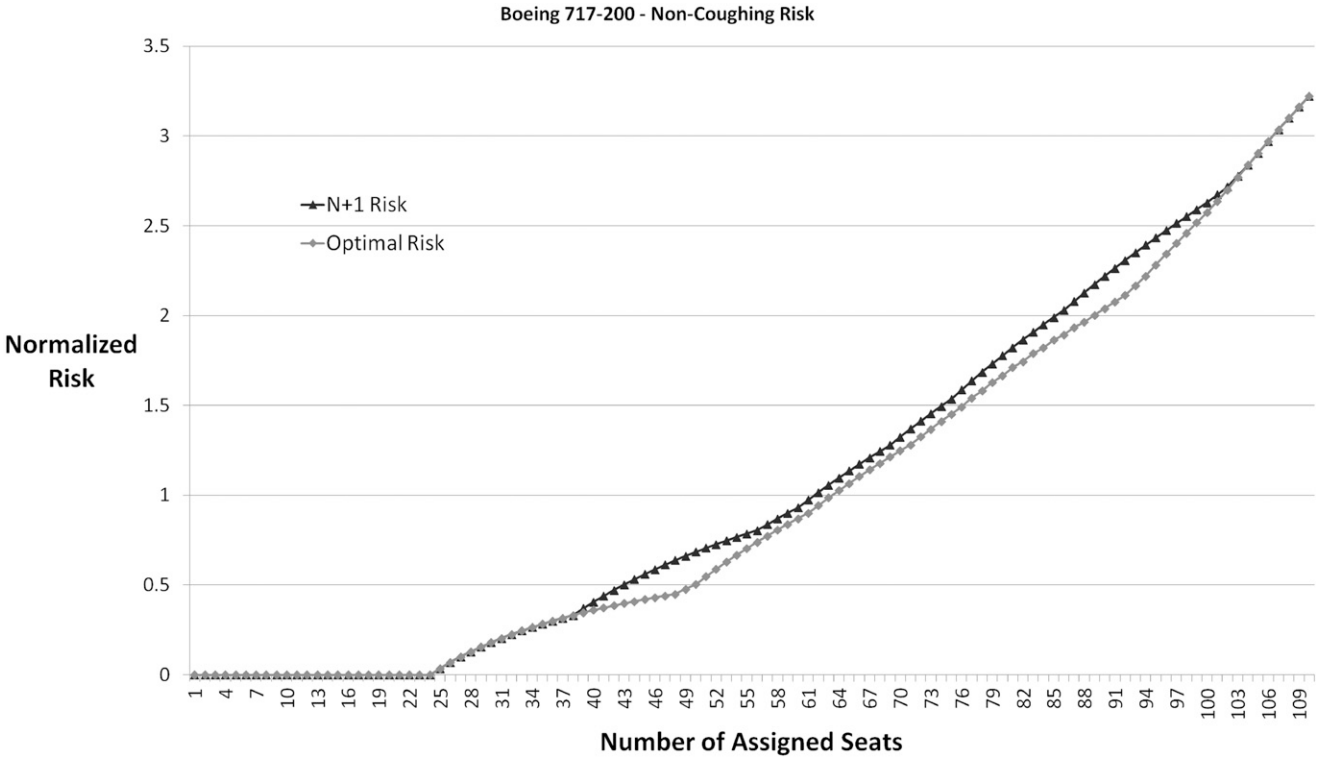

Figure 14. *N* + 1-Normalized Risk Relative to the Optimum Normalized Risk for Each Number of Passengers, Using the Noncoughing Model

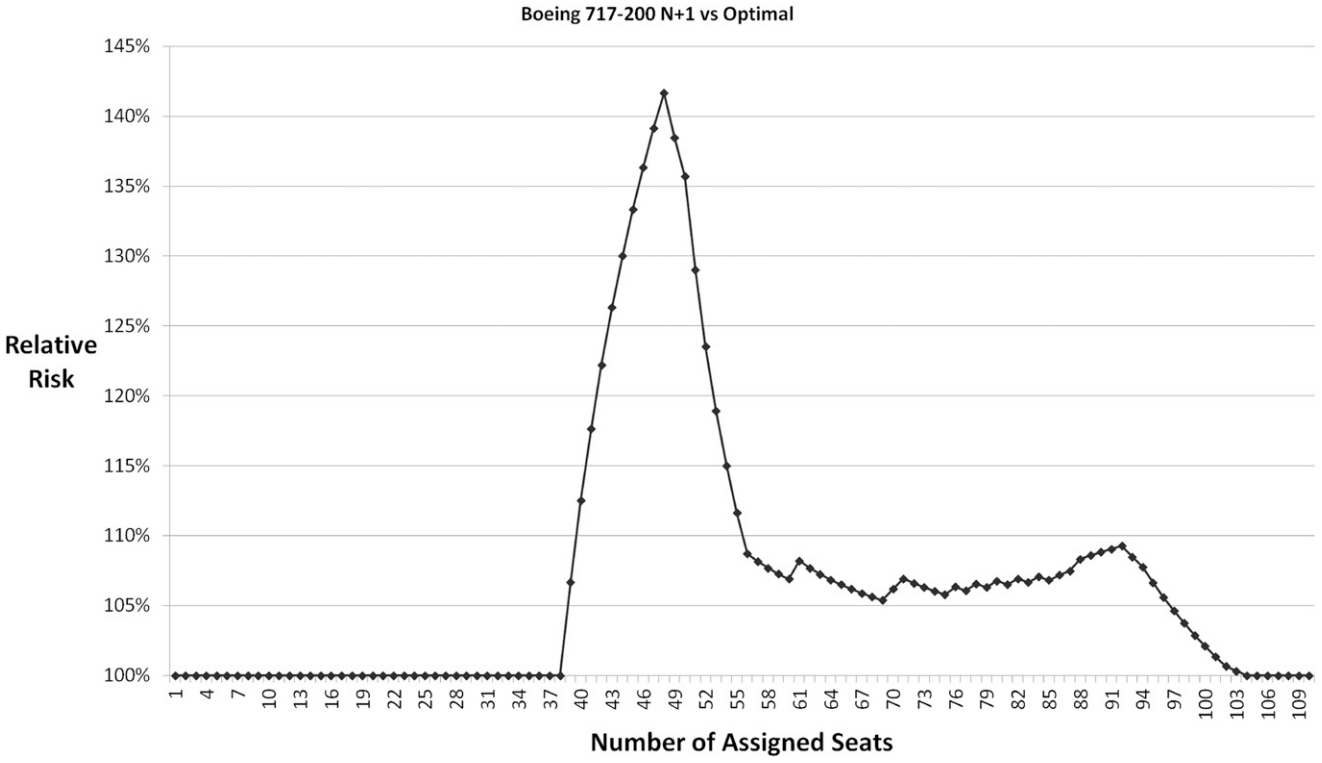

Figure 15. Crossover Risk Comparison

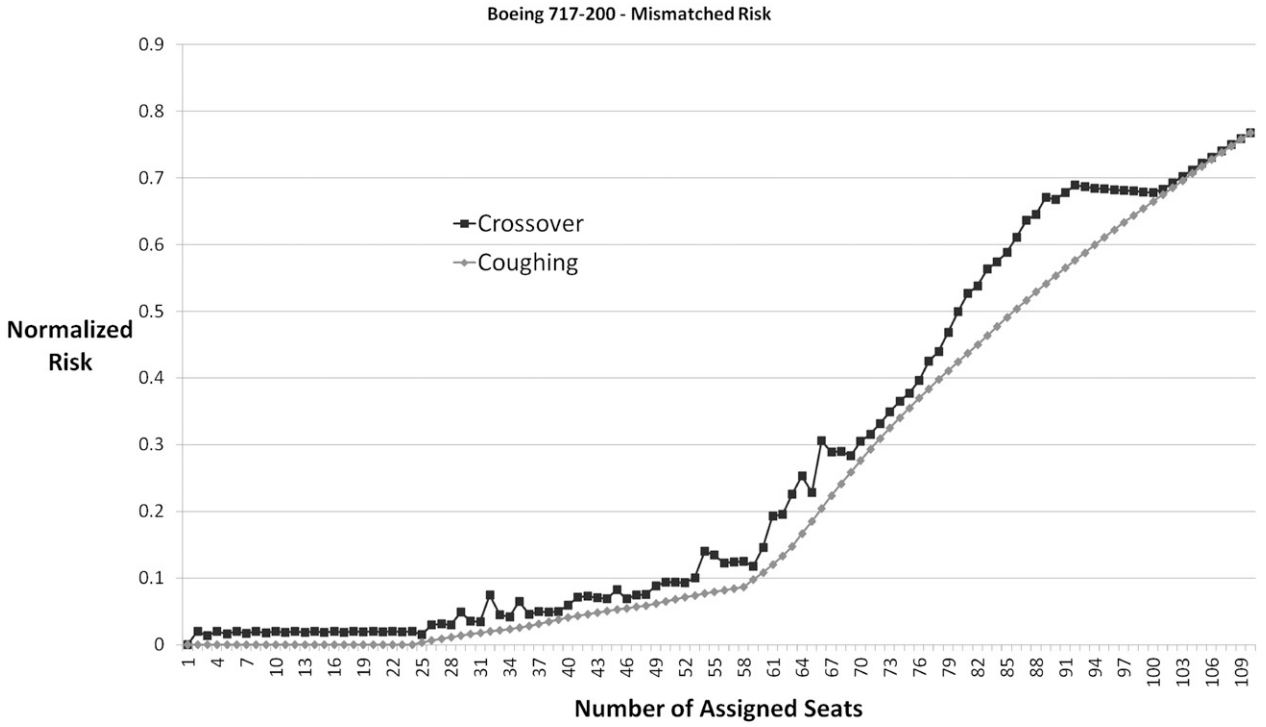

Note. Crossover is an optimal noncoughing seating arrangement with risk calculated using the coughing risk model, compared against the optimal coughing seating arrangement.

There are no risk models available for SARS-CoV-2 virus transmission on aircraft to date. As such, we rely on the available influenza risk models. Because ASAP only considers risks that are included in the input graphs, developing risk models specific to SARS-CoV-2 would produce ASAP seating arrangements that better minimize the risks of SARS-CoV-2 secondary infections compared with using influenza risks as a proxy. Moreover, transmission risks can be further reduced with the development of risk models tailored to each aircraft's ECS.

Acknowledgments

The authors thank the editor-in-chief and the anonymous reviewers for their comments that resulted in a significantly improved manuscript.

References

Air Transport Bureau (2020) Effects of novel coronavirus (Covid-19) on civil aviation: Economic impact analysis. Report, International Civil Aviation Organization, Montréal.

Azar AM II (2020) Determination that a public health emergency exists. Accessed October 9, 2020, https://www.phe.gov/emergency/news/healthactions/phe/Pages/2019-nCoV.aspx.

Chen J, He H, Cheng W, Liu Y, Sun Z, Chai C, Kong Q, et al (2020) Potential transmission of SARS-CoV-2 on a flight from Singapore to Hangzhou, China: An epidemiological investigation. *Travel Medicine Infectious Disease* 36(July–August):101816.

Delta Air Lines, Inc. (2020) Coronavirus travel: FAQs. Accessed September 18, 2020, https://www.delta.com/us/en/travel-update-center/coronavirus-travel-faqs.

Embraer (2020) Healthy journey. Accessed October 12, 2020, https://www.iata.org/contentassets/a1a361594bb440b1b7ebb632355373d1/embraer-healthy-journey.pdf.

Fargeon B (2020) Preview of Airbus' latest cabin air studies. Accessed October 12, 2020, https://www.iata.org/contentassets/a1a361594bb440b1b7ebb632355373d1/airbus-trust-airtravel.pdf.

Freedman DO, Wilder-Smith A (2020) In-flight transmission of SARS-CoV-2: A review of the attack rates and available data on the efficacy of face masks. *J. Travel Medicine* 27(8):taaa178.

Glover F, Kochenberger GA, Alidaee B (1998) Adaptive memory tabu search for binary quadratic programs. *Management Sci.* 44(3): 336–345.

Glover F, Kochenberger GA, Alidaee B, Amini M (1999) Tabu search with critical event memory: An enhanced application for binary quadratic programs. Voß S, Martello S, Osman IH, Roucairol C, eds. *Meta-Heuristics: Advances and Trends in Local Search Paradigms for Optimization* (Springer, Boston), 93–109.

Grinshpun SA, Haruta H, Eninger RM, Reponen T, McKay RT, Lee S-A (2009) Performance of an N95 filtering facepiece particulate respirator and a surgical mask during human breathing: Two pathways for particle penetration. *J. Occupational Environ. Hygiene* 6(10):593–603.

Hertzberg VS, Weiss H, Elon L, Si W, Norris SL, The FlyHealthy Research Team (2018) Behaviors, movements, and transmission of droplet-mediated respiratory diseases during transcontinental airline flights. *Proc. Natl. Acad. Sci. USA* 115(14):3623–3627.

Hochbaum DS (2004) Selection, provisioning, shared fixed costs, maximum closure, and implications on algorithmic methods today. *Management Sci.* 50(6):709–723.

Hochbaum DS, Pathria A (1997) Forest harvesting and minimum cuts: A new approach to handling spatial constraints. *Forest Sci.* 43(4):544–554.

International Air Transport Association (2020) Research points to low risk for COVID-19 transmission inflight. Accessed October 11, 2020, https://www.iata.org/en/pressroom/pr/2020-10-08-02/.

Khanh NC, Thai PQ, Quach HL, Thi NAH, Dinh PC, Duong TN, Mai LTQ, et al. (2020) Transmission of SARS-CoV 2 during long-haul flight. *Emerging Infectious Diseases* 26(11):2617–2624.

Kochenberger G, Alidaee B, Glover F, Wang H (2007) An effective modeling and solution approach for the generalized independent set problem. *Optim. Lett.* 1(1):111–117.

Nemhauser GL, Trotter LE (1975) Vertex packings: Structural properties and algorithms. *Math. Programming* 8(1):232–248.

Nir-Paz R, Grotto I, Strolov I, Salmon A, Mandelboim M, Mendelson E, Regev-Yochay G (2020) Absence of in-flight transmission of SARS-CoV-2 likely due to use of face masks on board. *J. Travel Medicine* 27(8):taaa117.

Pallini T (2020) I flew on the 4 biggest US airlines during the pandemic to see which is handling it best, and found one blew the rest out of the water. *Business Insider* (July 5), https://www.businessinsider.com/what-to-expect-when-flying-on-united-american-delta-southwest-during-pandemic-comparison-2020-7.

Pombal R, Hosegood I, Powell D (2020) Risk of COVID-19 during air travel. *J. Amer. Medical Assoc.* 324(17):1798.

Reuters (2020) Southwest extends limited seating on flights through September. *Reuters* (June 16), https://www.reuters.com/article/us-health-coronavirus-southwest-idUSKBN23N3GI.

Salari M, Milne RJ, Delcea C, Kattan L, Cotfas LA (2020) Social distancing in airplane seat assignments. *J. Air Transport Management* 89(October):101915.

Sherali HD, Smith JC (2006) A polyhedral study of the generalized vertex packing problem. *Math. Programming* 107(3):367–390.

Speake H, Phillips A, Chong T, Sikazwe C, Levy A, Lang J, Scalley B, et al. (2020) Flight-associated transmission of severe acute respiratory syndrome coronavirus 2 corroborated by whole-genome sequencing. *Emerging Infectious Diseases* 26(12):2872–2880.

Sze GNT, Wan MP, Chao CYH, Wei F, Yu SCT, Kwan JKC (2008) A methodology for estimating airborne virus exposures in indoor environments using the spatial distribution of expiratory aerosols and virus viability characteristics. *Indoor Air* 18(5):425–438.

Tang JW, Liebner TJ, Craven BA, Settles GS (2009) A schlieren optical study of the human cough with and without wearing masks for aerosol infection control. *J. Roy. Soc. Interface* 6(Supplement 6):S727–S736.

Tarjan RE, Trojanowski AE (1977) Finding a maximum independent set. *SIAM J. Comput.* 6(3):537–546.

Trump DJ (2020) Proclamation on suspension of entry as immigrants and nonimmigrants of persons who pose a risk of transmitting 2019 novel coronavirus. Accessed October 9, 2020, https://www.whitehouse.gov/presidential-actions/proclamation-suspension-entry-immigrants-nonimmigrants-persons-pose-risk-transmitting-2019-novel-coronavirus/.

Wan MP, To GNS, Chao CYH, Fang L, Melikov A (2009) Modeling the fate of expiratory aerosols and the associated infection risk in an aircraft cabin environment. *Aerosol Sci. Tech.* 43(4):322–343.

World Health Organization (2021) COVID-19 weekly epidemiological update. Accessed January 3, 2021, https://www.who.int/docs/default-source/coronaviruse/situation-reports/20201229_weekly_epi_update_con_20_cleared.pdf.

Yang N, Shen Y, Shi C, Ma AHY, Zhang X, Jian X, Wang L, et al (2020) In-flight transmission cluster of COVID-19: A retrospective case series. *Infectious Diseases* 52(12):891–901.

Zhang L, Li Y (2012) Dispersion of coughed droplets in a fully-occupied high-speed rail cabin. *Building Environ.* 47(January):58–66.